Phosphate Analogues as Probes of the Catalytic Mechanisms of MurA and AroA, Two Carboxyvinyl Transferases†

Fuzhong Zhang‡ and Paul J. Berti*,‡,§

Department of Chemistry, Department of Biochemistry and Biomedical Sciences, and Antimicrobial Research Centre, McMaster University, 1280 Main Street West, Hamilton, Ontario L8S 4M1, Canada

Received January 29, 2006; Revised Manuscript Received March 21, 2006

ABSTRACT: The role in catalysis of phosphate with AroA (enolpyruvyl shikimate 3-phosphate synthase) and MurA (enolpyruvyl UDP-GlcNAc synthase) was probed using phosphate analogues and an AroA mutant. Phosphate, the second reaction product, increases the reactivity of the enolpyruvyl products (EP-OR's) ~10^5-fold in the reverse reaction, forming phosphoenolpyruvate and R-OH (shikimate 3-phosphate or UDP-GlcNAc). Phosphate is intrinsically unreactive with EP-OR, raising the question of how AroA and MurA promote EP-OR reactivity. Eleven phosphate analogues were examined. All those with tetrahedral geometries bound with AroA, except sulfate, while no nontetrahedral analogues did. Arsenate, vanadate, and fluorophosphate caused reactions of AroA and MurA with EP-OR's, yielding pyruvate and R-OH. Their k_{cat}/K_M values relative to phosphate were similar for both enzymes, ca. 100-fold worse for arsensate, 200-fold worse for vanadate, and 5000-fold worse for fluorophosphate, implying similar interactions with both enzymes. Examination of the arsenate-promoted reactions using [3′-^{3}H]EP-OR's, ^2H_2O, and $H_2{}^{18}O$ provided evidence of an arseno-tetrahedral intermediate, analogous to the natural tetrahedral intermediate, proceeding to arsenoenolpyruvate, which spontaneously broke down to pyruvate and arsenate. The only physicochemical property that appeared to be essential for reactivity of the analogues was the presence of a proton. Titration of the intrinsic tryptophan fluorescence of the weakly active AroA mutant, Asp313Ala (D313A), demonstrated a fluorescence decrease upon enolpyruvyl shikimate 3-phosphate (EPSP) binding, and a further decrease upon binding of phosphate or arsenate to AroA_D313A·EPSP, suggesting a further conformational change. We are hopeful that understanding enzyme−phosphate interactions will make it possible to design inhibitors that can use the high endogenous phosphate concentration in bacteria to enhance inhibitor binding.

AroA[1] (EPSP synthase) (*1*, *2*) and MurA (UDP-GlcNAc enolpyruvyl transferase) (*3*, *4*) catalyze carboxyvinyl transfer. The enolpyruvyl products, EP-OR, of the forward reaction are EPSP and EP-UDP-GlcNAc (Scheme 1). AroA is part of the shikimate pathway leading to aromatic compounds in bacteria, parasites, and plants and is the target of glyphosate, a herbicide (*5*, *6*). MurA catalyzes the first committed step in peptidoglycan biosynthesis and is the target of fosfomycin, an antibiotic (*7*−*9*). They are homologous (*10*, *11*) and have been the subject of numerous mechanistic and structural studies (*1*, *2*, *8*, *10*−*45*). Nonetheless, important mechanistic questions remain; even such basic information as the identity of the catalytic residues is controversial (*38*, *39*, *41*, *44*).

Scheme 1

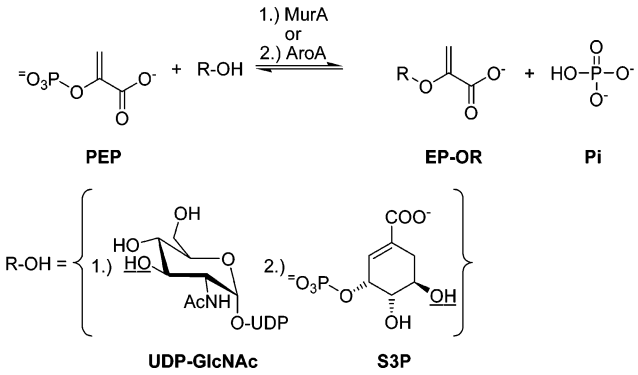

The reactions proceed via an addition−elimination pathway through a noncovalent tetrahedral intermediate, THI (*18*, *32*) (Scheme 2). Both the addition and elimination steps appear to pose significant catalytic challenges, yet they proceed smoothly, with k_{cat} values of 57 s^{-1} (AroA) (*46*) and 4 s^{-1} (MurA) (*28*) in the forward reaction and 13 s^{-1} (AroA) (*19*) in the reverse reaction. In the first step of both the forward and reverse reactions, the nonbasic C3′ atom must be protonated and nucleophilic attack by a poor

† This work was supported by the Canadian Institutes of Health Research.

* To whom correspondence should be addressed. Telephone: (905) 525-9140, ext. 23479. Fax: (905) 522-2509. E-mail: berti@mcmaster.ca.

‡ Department of Chemistry and Antimicrobial Research Centre.

§ Department of Biochemistry and Biomedical Sciences.

[1] Abbreviations: AroA, 5-enolpyruvyl shikimate 3-phosphate synthase; $AroA_{H6}$, AroA containing a C-terminal His_6 sequence; DTT, dithiothreitol; EP-OR, either EPSP or EP-UDP-GlcNAc; EPSP, 5-enolpyruvyl shikimate 3-phosphate; EP-UDP-GlcNAc, enolpyruvyl uridine diphospho *N*-acetylglucosamine; $K_{d,L}$, equilibrium dissociation constant of the enzyme with ligand L; KIE, kinetic isotope effect; LDH, lactate dehydrogenase; MurA, UDP-GlcNAc enolpyruvyl transferase; NADH, nicotinamide adenine dinucleotide; NPA, natural population analysis; PEP, phosphoenolpyruvate; S3P, shikimate 3-phosphate; THI, tetrahedral intermediate; UDP-GlcNAc, uridine diphosphate *N*-acetylglucosamine; TS, transition state.

10.1021/bi0601914 CCC: $33.50
Published on Web 04/20/2006

Scheme 2

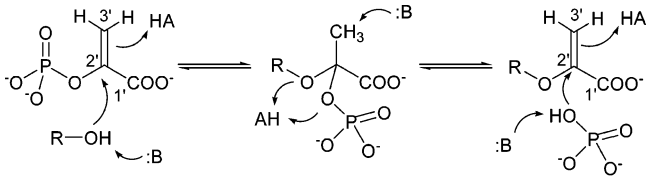

nucleophile, either a hydroxyl or a phosphate, must occur. The mechanism of these steps is not known. MurA and AroA hydrolyze EP-OR's slowly in the absence of phosphate, with a k_{cat} value of $\sim 5 \times 10^{-4}$ s^{-1} (*15*). Similarly, in the forward reaction, PEP is hydrolyzed slowly, if at all, but the correct reaction is fast in the presence of S3P or UDP-GlcNAc. In both cases, either phosphate or R-OH is required to promote protonation at C3′ and/or activate the nucleophile.

To probe the role of phosphate in catalysis, we studied the reverse reactions of AroA and MurA in the presence of phosphate analogues. Phosphate analogues have often been used as mechanistic probes for both P−O bond-cleaving enzymes (*47*−*55*) and C−O bond-cleaving enzymes (*56*−*62*).

We found that many phosphate analogues bound to AroA, but only $HAsO_4^{2-}$, $H_2VO_4^-$, and FPO_3^{2-} could promote catalysis, causing breakdown of EP-OR to pyruvate and R-OH. The same three phosphate analogues activated MurA. The arsenate-promoted reaction was studied in detail and evidence found for arseno-tetrahedral intermediates (arseno-THIs), similar to the natural reaction. Fluorescence titrations indicated that AroA undergoes conformational changes upon binding of phosphate or arsenate to the AroA·EPSP complex.

EXPERIMENTAL PROCEDURES

General

$H_2{}^{18}O$ was from Cambridge Isotope Laboratories, and [^{3}H]-water and [1′-^{14}C]pyruvate were from American Radiolabeled Chemicals. Other reagents were biotech or reagent grade from Sigma-Aldrich or Bioshop Canada (Burlington, ON). Shikimate 3-phosphate (S3P), EPSP and EP-UDP-GlcNAc, recombinant *Escherichia coli* MurA, $AroA_{H6}$ (AroA bearing a C-terminal His_6 sequence), and the $AroA_{H6}$_Asp313Ala (D313A) mutant were prepared as described previously (*43*, *45*). The His tag sequence has been shown to have a negligible effect on AroA's kinetic behavior.

[3′-^{3}H]EP-OR

A 200 μL solution containing 10 mM UDP-GlcNAc or S3P, 10 mM PEP, 50 mM Tris-HCl (pH 7.5), and 1 μM MurA or AroA was prepared in ^3H_2O (200 μCi) and incubated at room temperature for 12 h. After the reaction was quenched with 200 mM KOH and the mixture extracted with 3×200 μL of $CHCl_3$ to precipitate and remove protein, the product was separated by anion exchange on a Q-Sepharose column (20 mL column volume, Amersham Biosciences) with a gradient of 100 to 700 mM NH_4HCO_3 (pH 10.0) over 60 min, at 2 mL/min; 99% of the unreacted ^3H_2O eluted in the first 6 min. [3′-^{3}H]EP-OR's were collected and lyophilized by adding 3×3 mL of water.

Arsenate/Enzyme-Catalyzed EP-OR Breakdown

HPLC Analysis of Products. To a 200 μL reaction mixture containing 750 μM EP-OR and 8.5 μM enzyme in 50 mM Tris-HCl (pH 7.5) was added 40 μM sodium arsenate. After 2 h, the reaction mixture was separated by anion exchange chromatography (Mono-Q, 1 mL column volume, Amersham Biosciences) with a buffer containing 10 mM NH_4Cl (pH 10.0) and a gradient from 10 to 500 mM KCl over 15 column volumes with a flow rate of 0.5 mL/min and dual-wavelength absorbance detection at 260 and 240 nm for all reactions. Standards eluted at the following times: UDP-GlcNAc at 11.5 min, PEP at 16.2 min, EP-UDP-GlcNAc at 20.0 min, S3P at 13.4 min, and EPSP at 22.5 min. Concentrations were calculated from peak areas, with a relative molar absorptivity ratio of 0.01:1:1 for the PEP/UDP-GlcNAc/EP-UDP-GlcNAc mixture at 260 nm and 1:0.59:2.1 for the PEP/S3P/EPSP mixture at 240 nm. Control experiments without arsenate, and without enzyme or arsenate, were performed under the same conditions.

Radioactivity Assay. Sodium arsenate (200 μM) was added to 0.33 μM [1′-^{14}C]EP-OR (27 mCi/mmol), 20 μM enzyme, and 50 mM Tris-HCl (pH 7.5) in a volume of 100 μL. The reaction mixture was incubated for 30 min, and products were separated as described above; however, fractions were collected every 45 s, and the amount of ^{14}C in each fraction was determined by scintillation counting.

Lactate Dehydrogenase (LDH) Reaction. To confirm that the presumed pyruvate product was being formed, LDH was used in a spectrophotometric assay to reduce pyruvate to lactate. EP-OR breakdown reactions were set up with 0.4 mM EP-OR, 2 mM sodium arsenate, 0.2 μM enzyme, and 50 mM Tris-HCl (pH 7.5) in a volume of 500 μL. After 30 min, the reaction was quenched and the mixture extracted with 3×500 μL of $CHCl_3$. A 10 μL aliquot was analyzed by HPLC to ensure EP-OR breakdown was complete. To the remaining reaction solution was added 0.1 mM NADH to a total volume of 1 mL in a cuvette. LDH (1 unit) was added, and A_{340} was monitored, with a $\Delta\epsilon_{340}$ of 6220 M^{-1} cm^{-1} (*63*).

Kinetics of EP-OR Breakdown

To estimate k_{cat}/K_M for phosphate analogues, enzymes were incubated with EP-OR at concentrations much greater than the K_M and at phosphate analogue concentrations lower than the K_M. Initial velocities (v_0) were measured, and apparent k_{cat}/K_M values were calculated using eq 1:

$$v_0 = k_{cat}/K_M[\text{analogue}][\text{E·EP-OR}] \quad (1)$$

Both enzymes were assumed to follow a sequential bi-bi mechanism with random substrate binding with the phosphate analogues (*19*, *46*). Reaction mixtures (100 μL) containing 333 μM EP-UDP-GlcNAc or 750 μM EPSP, 8.5 μM MurA or 34 μM AroA, and 75−150 μM phosphate analogues in 50 mM Tris-HCl (pH 7.5) were incubated for up to 80 min. The products were then separated by anion exchange chromatography as described above, and peaks were quantified. For some reactions, 0.2−2 μM [1′-^{14}C]EPSP was added, and radioactivity in pyruvate and EPSP was measured.

Mechanism of Arsenate/Enzyme-Catalyzed EP-OR Breakdown

Hydrolysis in $H_2{}^{18}O$. Arsenate-promoted enzymatic EP-OR hydrolysis was performed in $H_2{}^{18}O$ to determine the site of nucleophilic attack by water. AroA (48 μM) or MurA

(34 μM) was added to a reaction mixture containing 0.5 mM EP-OR and 0.25 mM sodium arsenate in 86 μL of $H_2{}^{18}O$ at pH 7.5 in a volume of 100 μL. After 5−28 min, the reaction was quenched with $CHCl_3$ extraction and the mixture analyzed immediately by mass spectrometry. Control experiments were performed either without EP-OR or enzyme or in $H_2{}^{16}O$.

Tritium Release. The formation of arseno-THI was tested by detecting any [^{3}H]water released upon [3′-^{3}H]EP-OR breakdown. In MurA-catalyzed reactions, 12 mM EP-UDP-GlcNAc containing 500 cpm of [3′-^{3}H]EP-UDP-GlcNAc, 20 mM sodium arsenate, 40 μM MurA, 14 mM NADH, and 0.05 mg/mL LDH was incubated in 50 mM Tris-HCl (pH 7.5). Pyruvate was converted to lactate with LDH to prevent ^{3}H exchange with solvent. A control experiment without arsenate was carried out in parallel. The reactions were quenched after 15 min with 120 mM HCl and the mixtures extracted with 3 × 200 μL of $CHCl_3$. The aqueous solution was then diluted to 4 mL and evenly divided into two scintillation vials. One vial was lyophilized, followed by repeated lyophilization and addition of regular water. Radioactivity in each vial was counted for 3 × 10 min, and radioactivity loss in the lyophilized vial was determined. AroA was tested in the same way, with reaction mixtures containing 1.6 mM EPSP with 500 cpm of [3′-^{3}H]EPSP and 100 μM AroA, and reactions were quenched after 6 min.

Enolpyruvyl ^{2}H Exchange with Solvent

Hydron exchange at C3′ was studied by carrying out reactions in ^2H_2O. For arsenate/MurA reactions, EP-UDP-GlcNAc and arsenate were lyophilized and then redissolved in ^2H_2O, followed by addition of MurA and a volatile buffer, NH_4HCO_3 (pH 7.5). Final concentrations were as follows: 225 μM EP-UDP-GlcNAc, 8 mM sodium arsenate, 7.7 μM MurA, 50 mM NH_4HCO_3 (in 200 μL of 95% ^2H_2O). The reaction was quenched with 50% NH_4OH at 50% completion, as monitored by HPLC, and the mixture extracted with $CHCl_3$, and then the aqueous layer was repeatedly lyophilized and redissolved in H_2O at least five times before being dissolved in a 50% MeOH/2.5% formic acid solution and analyzed by negative ion electrospray mass spectrometry. Vanadate/MurA reactions were carried out in the same way except using 225 μM EP-UDP-GlcNAc, 2 mM vanadate, and 0.4 μM MurA.

^{2}H exchange was studied similarly for AroA-catalyzed reactions using 375 μM EPSP, 25−333 μM phosphate analogue, and 5.3−15 μM AroA in 50 mM NH_4HCO_3 (pH 7.5) in 200 μL of 95% ^2H_2O. Reactions were quenched with 50% NH_4OH for 1 min to 12 h. Sample preparation and mass spectrometry were as for the MurA reactions. Reaction with any contaminating phosphate was suppressed by adding 50 μM KCl, 50 μM $MgCl_2$, 300 μM ADP, and 0.2 unit of pyruvate kinase (PK) to synthesize ATP from any PEP formed from phosphate by AroA. Contaminating phosphate concentrations were very low and did not interfere with the ^2H_2O exchange experiments.

^{2}H incorporation was detected by negative ion mass spectrometry as the change in the intensity of the *m*/*z* *n*, *n* + 1, and *n* + 2 peaks for EPSP (*n* = 323) or EP-UDP-GlcNAc (*n* = 676). After correction for natural abundance isotopes, the fractional extent of ^{2}H incorporation, $f(^2H)$, was calculated using eq 2:

$$f(^2H) = \frac{I_{n+1} + 2I_{n+2}}{2(I_n + I_{n+1} + I_{n+2})} \quad (2)$$

where I_n is the intensity of the peak at a given *m*/*z* value. The ^{2}H exchange rate, k_{ex}, was calculated from a plot of $f(^2H)$ versus time at low extents of reaction and was compared with k_{rxn}, the fractional extent of EP-OR breakdown, under the same conditions. Parallel reactions were run without the phosphate analogues, and the k_{ex} and k_{rxn} values were corrected for exchange and EP-OR hydrolysis without the analogue.

Fluorescence Titrations

Equilibrium dissociation constants ($K_{d,L}$) for binding of phosphate analogues to $AroA_{H6}$ were determined using steady state fluorescence titrations in a 2 mL quartz cuvette at 25 °C, with a λ_{ex} of 280 nm and a λ_{em} of 360 nm. Aliquots of 0.5−10 μL of ligand (phosphate or an analogue) were added to 0.5 or 1 μM enzyme in 50 mM Tris-HCl (pH 7.5) and 1 mM DTT, and the fluorescence was read for 60 × 0.5 s and averaged. Ligand was added until no further fluorescence change was observed. The temperature of each sample was equilibrated in the spectrofluorometer for 20 min before the beginning of each titration. After correction for dilution, fluorescence intensity was plotted versus total ligand concentration, [L], and fitted to eq 3:

$$F = F_0 - \frac{(F_0 - F_{inf})\left[\frac{([E]_0 + [L] + K_{d,L}) - \sqrt{([E]_0 + [L] + K_{d,L})^2 - 4[E]_0[L]}}{2}\right]}{[E]_0} \quad (3)$$

where F was the observed fluorescence intensity, $[E]_0$ was the total enzyme concentration, F_0 and F_{inf} were the fitted fluorescence intensities at zero and infinite [L], respectively, and $K_{d,L}$ was the fitted equilibrium ligand dissociation constant.

Thiophosphate and monomethyl phosphate binding was competitive with EPSP, which was also studied by fluorescence titrations. Thiophosphate (0.5−2 mM) or monomethyl phosphate (11.5−115 mM) was equilibrated with $AroA_{H6}$ for 30 min in the spectrofluorometer to achieve a constant temperature and then titrated with EPSP as described above. The apparent $K_{d,EPSP}$ was fitted at each analogue concentration, and $K_{d,analogue}$ for each analogue was fitted to eq 4:

$$K_{d,EPSP}(\text{apparent}) = K_{d,EPSP}(1 + [\text{analogue}]/K_{d,analogue}) \quad (4)$$

RESULTS

Eleven phosphate analogues were tested (Table 1); three were able to promote EP-OR breakdown to pyruvate and R-OH: arsenate ($HAsO_4^{2-}$), vanadate ($H_2VO_4^-$), and monofluorophosphate (FPO_3^{2-}).

Equilibrium Dissociation Constants

Equilibrium dissociation constants, $K_{d,L}$, for phosphate and some analogues were determined by direct fluorescence titration with $AroA_{H6}$, His_6-tagged *E. coli* AroA (Figure 1a

Table 1: Interactions of Phosphate and Phosphate Analogues with MurA and AroA[a]

	HPO_4^{2-}	$HAsO_4^{2-}$	$H_2VO_4^-$	FPO_3^{2-}	SO_4^{2-}	WO_4^{2-}	$MePO_3^{2-}$	$MeOPO_3^{2-}$	$HSPO_3^{2-}$
MurA k_{cat}/K_M (M^{-1} s^{-1})[b]	$(2.0 \pm 0.5) \times 10^4$	150 ± 30	90 ± 40	3.3 ± 0.6	nd[c]	nd[c]	nd[c]	nd[c]	nd[c]
MurA specificity ratio[d]	1	130	220	6000					
MurA k_{ex}/k_{rxn}[e]		0.67 ± 0.04	0.12 ± 0.05		nd[c]	nd[c]			
AroA k_{cat}/K_M (M^{-1} s^{-1})[b]	$(4.5 \pm 0.9) \times 10^3$	77 ± 15	20 ± 4	1.2 ± 0.2	nd[c]	nd[c]	nd[c]	nd[c]	nd[c]
AroA specificity ratio[d]	1	60	220	3800					
AroA k_{ex}/k_{rxn}[e]		1.4 ± 0.1	0.4 ± 0.1						
AroA K_d (mM)	4.8 ± 0.5	5.4 ± 0.6	0.4 ± 0.2[f]	0.6 ± 0.2	[g]	17 ± 5[h]	148 ± 10	$23 \pm 2/22 \pm 2$[i]	0.21 ± 0.01[i]
bond length (Å)[j]	1.50	1.66	1.68	1.49 (P−F bond, 1.65)	1.48	1.77	1.50	1.52	1.51 (P−S bond, 2.13)
[dianion]/[monoanion][k]	2	4	0.03	500	3×10^5	600	0.6	16	50

[a] In addition, AlF_4^-, HCO_3^-, and NO_3^- were tested, but none interacted detectably with MurA or AroA. [b] k_{cat}/K_M for reaction to R-OH + PEP (with phosphate) or R-OH + pyruvate (with analogues). [c] Not detectable ($k_{cat}/K_M < 0.04$ M^{-1} s^{-1}). [d] $(k_{cat}/K_M)_{phosphate}/(k_{cat}/K_M)_{analogue}$. [e] k_{ex}/k_{rxn} is the rate of ^2H incorporation, k_{ex}, divided by the rate of EP-OR breakdown, k_{rxn}, in the presence of a phosphate analogue, corrected for exchange and breakdown in the absence of the analogue. Under the reaction conditions, k_{ex} without each phosphate analogue was 17% (AroA/$HAsO_4^{2-}$), 46% (AroA/$H_2VO_4^-$), 47% (MurA/$HAsO_4^{2-}$), and 40% (MurA/$H_2VO_4^-$) of k_{ex} in the presence of the analogue. [f] K_{M,VO_4} for vanadate-promoted EPSP hydrolysis. [g] No detectable fluorescence change up to 100 mM. [h] K_{i,WO_4} was determined from inhibition of the $AroA_{H6}$-catalyzed reaction of EPSP and phosphate, assuming that inhibition was competitive with respect to phosphate. [i] From the variation in $K_{d,EPSP}$ as determined by fluorescence titration, with variable [$MeOPO_3^{2-}$] or [$HPSO_3^{2-}$]. The Trp fluorescence change due to $HPSO_3^{2-}$ binding was too small for direct determination of $K_{d,HPSO_3}$. [j] Bond length between the central atom and the charged oxygen (from Cambridge Structural Database). [k] The [dianion]/[monoanion] ratio was calculated from pK_{a2} using the Henderson−Hasselbach equation, and pK_{a2} values from refs *64*−*67*.

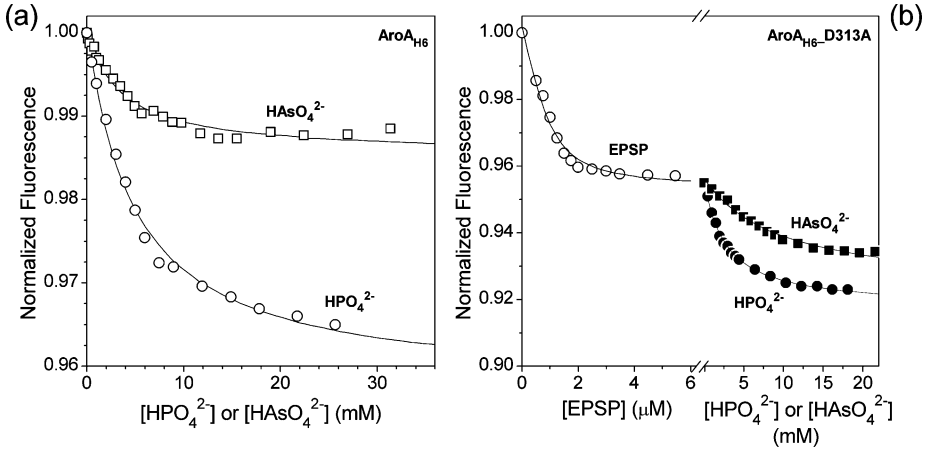

FIGURE 1: (a) Fluorescence titrations of binding of $HAsO_4^{2-}$ and HPO_4^{2-} to 0.5 μM $AroA_{H6}$. Solid lines indicate calculated curves from fitting fluorescence data to eq 3 (Table 1). (b) Fluorescence titrations of 0.5 μM $AroA_{H6}$_D313A with EPSP (○) followed by HPO_4^{2-} (●) in the same sample. $HAsO_4^{2-}$ (■) was titrated into $AroA_{H6}$_D313A·EPSP in a separate experiment. Solid lines indicate calculated curves from fitting fluorescence data to eq 3.

and Table 1). Ligands that bind AroA, including EPSP and {S3P+glyphosate}, cause a decrease in Trp fluorescence that has been correlated with the two AroA domains moving closer together and closing down the active site (*14*, *26*). $K_{d,EPSP}$ with $AroA_{H6}$ was 1.6 ± 0.1 μM, compared with 1 μM with wild-type AroA (*14*). K_{d,HPO_4} (4.8 mM) was similar to values measured previously with wild-type AroA, which range from 0.7 mM (*1*) to 14 mM (*19*) under various conditions, and K_M = 4.4 mM (*19*). The fluorescence change caused by thiophosphate, $HSPO_3^{2-}$, was too small to determine $K_{d,HSPO_3}$ by direct fluorescence titration. Instead, $K_{d,EPSP}$(apparent) was determined by fluorescence titration in the presence of varying $HSPO_3^{2-}$ concentrations, and the value of $K_{d,HSPO_3}$ (0.21 mM) was found by fitting to eq. 4, as in previous reports (Figure 2) (*43*). With monomethyl phosphate, $MeOPO_3^{2-}$, $K_{d,MeOPO_3}$ values were determined by direct fluorescence titration and by application of eq 4, giving values of 22 and 23 mM, respectively. Fluorescence titrations could not be used with tungstate, WO_4^-, which quenched Trp fluorescence nonspecifically, giving the same titration curve with $AroA_{H6}$ as with *N*-acetyltryptophan. Tungstate inhibited the reverse AroA reaction (EPSP + phosphate → S3P + PEP), and K_{i,WO_4} was found to be 17 mM (Table 1), which was taken as K_{d,WO_4}. Vanadate, $H_2VO_4^-$, absorbed significantly at λ_{ex}, 280 nm, preventing fluorescence titrations. Instead, K_{M,H_2VO_4}, 0.4 mM, for the vanadate-promoted reaction was reported.

Several approaches were used in an attempt to detect sulfate binding or reactivity, given the fact that it should be one of the closest analogues of phosphate. There was no detectable binding to AroA by fluorescence titration with up to 100 mM sulfate. At 120 mM, it did not inhibit the reverse AroA reaction or EPSP hydrolysis by AroA alone, and it did not promote solvent ^2H exchange in ^2H_2O.

Fluorescence Titrations with $AroA_{H6}$_D313A

$AroA_{H6}$_D313A, a mutant with extremely low activity, experienced a decrease in fluorescence intensity similar to

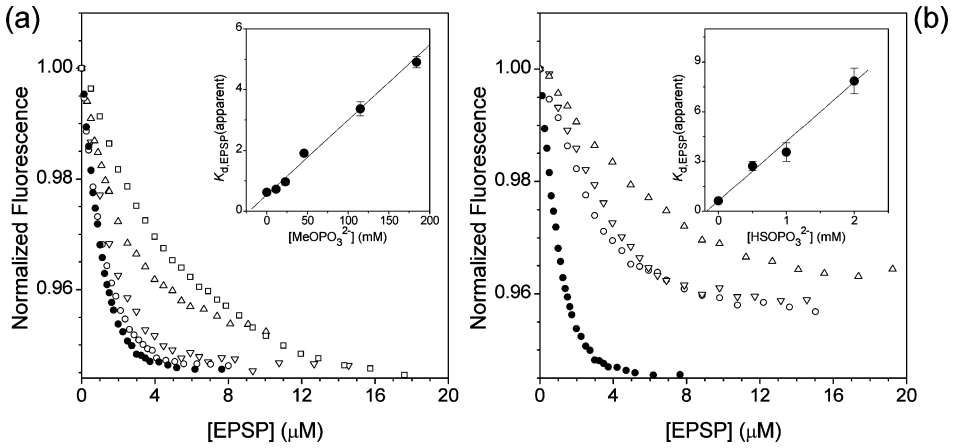

FIGURE 2: Estimation of $K_{d,MeOPO_3}$ and $K_{d,HSPO_3}$ from $K_{d,EPSP}$(apparent). (a) Fluorescence titration of 1 μM AroA$_{H6}$ with EPSP in the presence of varying amounts of $MeOPO_3^{2-}$: (●) 0, (○) 11.5, (▽) 23, (△) 115, and (□) 184 mM. The inset shows $K_{d,EPSP}$(apparent) vs [$MeOPO_3^{2-}$]. (b) Fluorescence titration of 1 μM AroA$_{H6}$ with EPSP in the presence of varying amounts of thiophosphate, $HSPO_3^{2-}$: (●) 0 (same data as part a), (○) 0.5, (▽) 1, and and (△) 2 mM. The inset shows $K_{d,EPSP}$(apparent) vs [$HSPO_3^{2-}$]. The reason for the smaller decrease in fluorescence at higher $HSPO_3^{2-}$ concentrations is not clear but may be related to the fact that $HSPO_3^{2-}$ binding on its own caused a negligible change in AroA fluorescence.

that of AroA$_{H6}$ when titrated with EPSP or phosphate, with K_d values of 0.6 ± 0.1 μM (Figure 1b) and 4.2 ± 0.5 mM (data not shown), respectively. Titration of AroA$_{H6}$_D313A·EPSP with phosphate revealed a second fluorescence change, with a K_{d,HPO_4} of 2.7 ± 0.1 mM (Figure 1b). Fluorescence titration of AroA$_{H6}$_D313A·EPSP with arsenate gave a $K_{d,HAsO_4}$ of 9 ± 1 mM (Figure 1b).

Phosphate and Analogue Binding Site

As both EPSP and EP-UDP-GlcNAc contain phosphate ester functional groups, it is possible that inorganic phosphate or analogues bound in those site in preference to the correct phosphate binding site. Although it is not possible to rigorously exclude this possibility, results with AroA$_{H6}$_D313A indicate that phosphate bound in its correct site. Asp313 is located in the active site, but not close to either the inorganic phosphate or phosphate monoester binding sites. Titrating AroA$_{H6}$_D313A with phosphate gave a fluorescence decrease similar in magnitude to that with AroA$_{H6}$, and a slightly lower K_{d,HPO_4} (4.2 mM). In the presence of 6 μM EPSP (10$K_{d,EPSP}$), there was a slight decrease in K_{d,HPO_4}, to 2.7 mM, consistent with tighter phosphate binding in the presence of EPSP, as observed previously (*19*). Thus, EPSP did not interfere with phosphate binding, providing some evidence that it bound in the correct site even in the absence of EPSP.

Kinetics of EP-OR Breakdown

The specificity constants (k_{cat}/K_M) for EP-OR breakdown were determined from the initial reaction velocities with different phosphate analogues (Table 1). It was possible to estimate $(k_{cat}/K_M)_{analogue}$ using eq 1 because phosphate analogue concentrations were less than $K_{d,analogue}$, while EP-OR concentrations were much greater than $K_{d,EP-OR}$ (750 μM EPSP and 333 μM EP-UDP-GlcNAc); cf. $K_{d,EPSP} = 0.6$ μM (this study) and $K_{d,EP-UDP-GlcNAc} \sim 1$ μM (*21*). Compared to the k_{cat}/K_M value with phosphate, k_{cat}/K_M with both enzymes decreased roughly 100-fold for arsenate, 200-fold for vanadate, and 5000-fold for fluorophosphate. For the analogues that did not promote hydrolysis, we can estimate an upper limit on k_{cat}/K_M of 0.04 M^{-1} s^{-1} based on the lack of detectable EP-OR breakdown (<1%) under the experimental conditions, that is, an at least 10^5-fold (AroA) to 5 × 10^5-fold (MurA) decrease.

Scheme 3

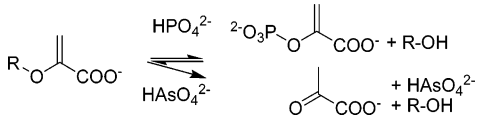

EP-OR Breakdown Products

As arsenate was the most effective analogue at promoting EP-OR breakdown, its reaction was characterized in detail. Arsenate-promoted enzymatic EP-OR degradation yielded pyruvate, arsenate, and R-OH (UDP-GlcNAc or S3P) (Scheme 3). The EP-OR's were not significantly degraded in the presence of enzyme alone under these conditions. The breakdown products were identified as follows. Arsenate-promoted EP-OR breakdown resulted in a new peak in anion exchange chromatograms with the same elution times and A_{260}/A_{240} ratios as UDP-GlcNAc (with MurA) (Figure 3) or S3P (with AroA), as well as the expected *m*/*z* values by mass spectrometry (data not shown). Reaction with [1′-^{14}C]EP-OR gave a radioactive peak that coeluted with standard pyruvate. Degrading 100 μM EPSP or EP-UDP-GlcNAc in the presence of arsenate and AroA or MurA yielded 97 ± 5 μM pyruvate, as detected by reaction with NADH and LDH. Incubating [1′-^{14}C]pyruvate with R-OH, arsenate, and enzyme yielded no detectable EP-OR, indicating that the reaction was effectively irreversible.

Mechanism of Arsenate-Promoted EP-OR Breakdown

Because several different reaction pathways could lead to pyruvate formation in the arsenate-promoted reactions, isotope labeling experiments using [3′-^{3}H]EP-OR, ^2H_2O, and $H_2{}^{18}O$ were used to probe the reaction (Tables 1 and 2 and Figures 4 and 5). With [3′-^{3}H]EP-OR, ^{3}H would be released if C3′ were protonated, and then deprotonated, as during THI formation and breakdown, or reversible formation of a putative oxacarbenium ion, but not if water directly attacked EP-OR or the oxacarbenium ion while arsenate acted as a bystander (Figure 4). Incorporation of ^{2}H from ^2H_2O into EP-OR's would demonstrate reversible formation of arseno-

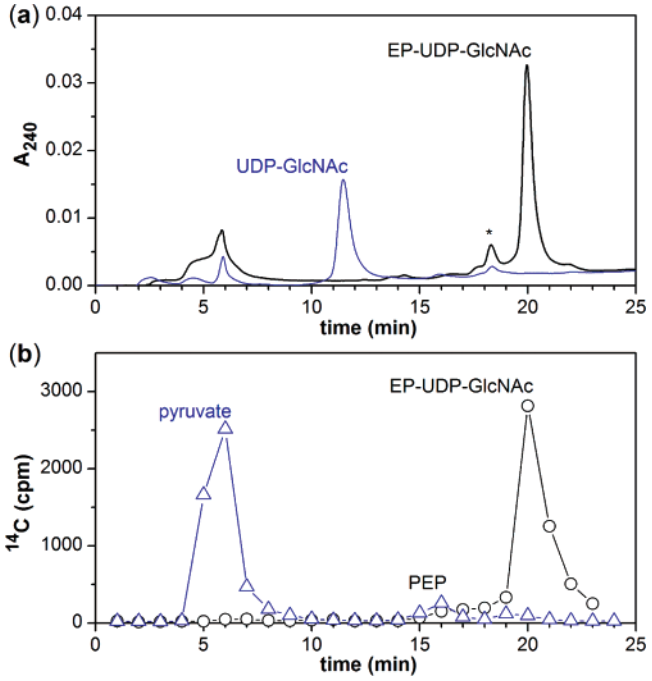

FIGURE 3: EP-UDP-GlcNAc breakdown products. Anion exchange chromatograms of reaction mixtures at 2 h. (a) A_{240} in the absence (black line) and presence (blue line) of $HAsO_4^{2-}$. (b) ^{14}C in 1 min fractions in the absence (○) and presence (△) of $HAsO_4^{2-}$. For panel a, the reaction mixture contained 750 μM EP-UDP-GlcNAc, 8.5 μM MurA, and 50 mM Tris-HCl (pH 7.5) with or without 40 μM $HAsO_4^{2-}$. The peak marked with an asterisk was UDP-MurNAc, a peptidoglycan biosynthesis intermediate present in all MurA preparations (*43*). For panel b, the reaction mixture contained 0.33 μM [1′-^{14}C]EP-UDP-GlcNAc, 20 μM MurA, and 50 mM Tris-HCl (pH 7.5) with or without 200 μM $HAsO_4^{2-}$. The small amount of [1′-^{14}C]PEP arises from the covalent PEP adduct present in all MurA preparations (*21*, *43*) and could be suppressed by the addition of pyruvate kinase and ADP.

THI and/or an oxacarbenium ion intermediate (Figure 4). As arsenate esters are unstable in water and undergo As−O bond cleavage (*56*, *68*), incorporation of ^{18}O into arsenate would demonstrate whether arsenate was participating in the reaction or was merely a bystander.

AroA Reactions. In arsenate/AroA reactions, [3′-^{3}H]EPSP breakdown released ^3H into solution (Table 2). Complete hydrolysis gave an observed fractional loss of ^3H, $\Delta f(^3H$ loss), of 0.23, indicating that at some point the EP-OR methylene was protonated, rotationally equilibrated, and then deprotonated. Assuming no isotope effect on deprotonation and full rotational equilibration of the $CH_2{}^3H$ group, one-third of ^3H would be expected to be removed; i.e., $\Delta f(^3H$ loss) would

Table 2: Release of ^3H from [3′-^{3}H]EP-OR's in Arsenate-Promoted Reactions

	$f(^3H$ loss)[a]		
enzyme, reactant	with $HAsO_4^{2-}$	without $HAsO_4^{2-}$	$\Delta f(^3H$ loss)[b]
AroA, [3′-^{3}H]EPSP	0.36 ± 0.03	0.13 ± 0.02	0.23 ± 0.05
MurA, [3′-^{3}H]EP-UDP-GlcNAc	0.23 ± 0.02	0.01 ± 0.03	0.22 ± 0.05

[a] $f(^3H$ loss) is the fraction of the total ^3H lost from the reaction mixture upon lyophilization, which corresponds to the loss of ^3H from [3′-^{3}H]EP-OR into water: $f(^3H\text{ loss}) = (^3H_{no-lyoph} - {}^3H_{lyoph})/{}^3H_{no-lyoph}$. [b] $\Delta f(^3H\text{ loss}) = f(^3H$ loss with $HAsO_4^{2-}) - f(^3H$ loss without $HAsO_4^{2-})$.

be 0.33. A modest kinetic isotope effect (KIE) on hydrogen extraction would account for the discrepancy from the expected value, though a large ^3H KIE might reasonably be expected. Indeed, a solvent ^2H KIE of almost 2 was observed previously for the AroA reaction at pH 6.25 (though there is no direct evidence that the observed KIE reflected protonation and/or deprotonation of the methyl group) (*69*, *70*). Assuming a large KIE on deprotonation, repeated protonation and/or deprotonation at C3′ would be required to account for the observed release of ^3H into solution. ^3H loss is consistent with (i) arseno-THI formation followed by R-OH elimination to form arsenoenolpyruvate (Figure 4), (ii) reversible formation of arseno-THI, or (iii) reversible formation of an oxacarbenium ion intermediate. If the newly formed methyl group rotates during the intermediate's lifetime, the catalytic acid can abstract ^3H.

Solvent ^2H exchange into the C3′ position was measured as k_{ex}/k_{rxn}, the ratio of ^2H exchange, k_{ex}, to EP-OR breakdown, k_{rxn}. With AroA and arsenate, k_{ex}/k_{rxn} was 1.7 (Table 1), implying either (i) reversible arseno-THI formation or (ii) reversible oxacarbenium ion intermediate formation before nucleophilic addition of $HAsO_4^{2-}$ (Table 1). Both possibilities are consistent with release of ^3H from [3′-^{3}H]EPSP.

AroA/arsenate reactions run in $H_2{}^{18}O$ resulted in incorporation of ^{18}O into arsenate (Figure 5b), indicating at least that arseno-THI and likely arsenoenolpyruvate (Figure 4) were formed, followed by nonenzymatic breakdown of the arsenate ester through As−O bond cleavage (*56*, *61*). There was little ^{18}O exchange in the absence of EPSP (Figure 5a). Repeated trips through the catalytic cycle formed $HAs^{16}O_2{}^{18}O_2^{2-}$ and $HAs^{16}O^{18}O_3^{2-}$, even though the reaction had not gone to completion. Dissociation and nonenzymatic breakdown of the arseno-THI would account for the observed incorporation of ^{18}O; however, given the extremely high affinity of AroA for the normal THI, its demonstrated ability to deprotonate C3′, and the fact that elimination of S3P is

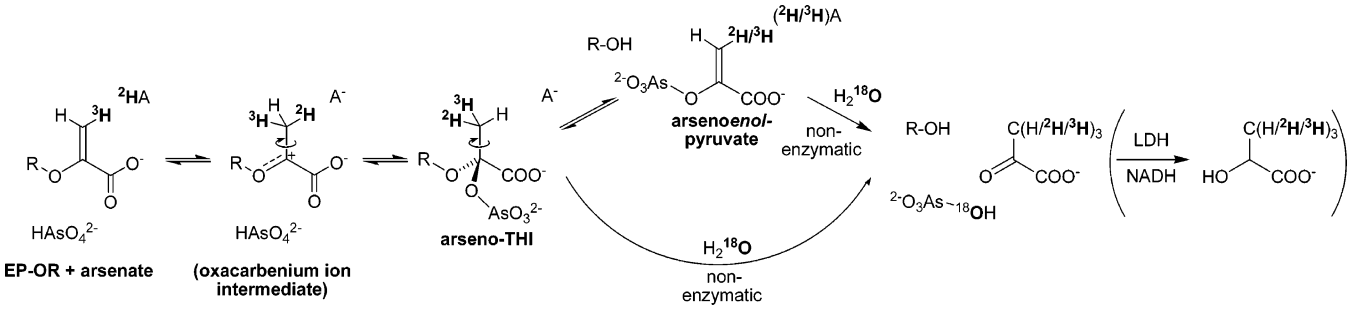

FIGURE 4: Isotope labeling experiments for arsenate-promoted reactions showing sources and potential fates of isotopic labels. Note that in any given experiment, only one isotopic label was used. Product pyruvate was reduced to lactate with LDH/NADH to prevent nonenzymatic hydron exchange. Spontaneous ^{18}O exchange into pyruvate was fast and therefore not useful diagnostically.

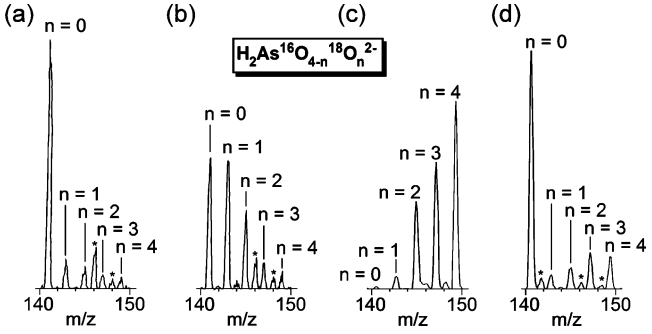

FIGURE 5: Arsenate ^{18}O exchange in arsenate-promoted EP-OR hydrolysis in 86% $H_2{}^{18}O$. (a) AroA + $HAsO_4{}^{2-}$, with incubation for 18 min. (b) AroA + $HAsO_4{}^{2-}$ + EPSP, after 18 min. EPSP was 70% hydrolyzed. (c) MurA + $HAsO_4{}^{2-}$, with incubation for 5 min. (d) MurA + $HAsO_4{}^{2-}$ + EP-UDP-GlcNAc, after 28 min. EP-UDP-GlcNAc was 70% hydrolyzed. Asterisks denote contaminants.

the same reaction with arseno-THI as with the normal THI, it is much more likely that AroA forms arsenoenolpyruvate. Nonenzymatic breakdown of arsenoenolpyruvate through As−O bond cleavage will then give ^{18}O incorporation.

MurA Reactions. The results with ^3H and ^2H labeling in the arsenate-promoted MurA reactions were similar to those for AroA reactions (Tables 1 and 2), indicating that C3′ of EP-UDP-GlcNAc was protonated, rotationally equilibrated, and then deprotonated. The fractional loss of ^3H, 0.22, was very similar to that of AroA, 0.23. Solvent ^2H exchange, as measured by k_{ex}/k_{rxn}, was slower than that of AroA but was still significant.

Incubation of MurA and arsenate in $H_2{}^{18}O$ caused extensive exchange (Figure 5c), indicating that arsenate was bound in an environment that rendered it more reactive. MurA contains a good nucleophile in the active site, Cys115, located near the phosphate binding site, that could conceivably interact with arsenate. Addition of 500 μM EP-UDP-GlcNAc largely suppressed ^{18}O exchange (Figure 5d). As [EP-UDP-GlcNAc] $\gg K_{d,EP-UDP-GlcNAc}$, MurA was saturated with EP-UDP-GlcNAc, and ^{18}O exchange in the MurA·$HAsO_4{}^{2-}$·EP-UDP-GlcNAc complex was much slower than in the MurA·$HAsO_4{}^{2-}$ complex. The lack of significant ^{18}O incorporation as EP-UDP-GlcNAc breakdown proceeded to 70% completion could indicate that arsenate was not participating in the breakdown reaction, i.e., that it was a bystander, or that the presumed arsenoenolpyruvate product was degraded through another pathway. This could include an arsenolactoyl adduct (**1**) analogous to the commonly observed phospholactoyl adduct (*21*, *43*), or MurA-catalyzed water attack on C2′ of arsenoenolpyruvate. MurA has a nanomolar $K_{M,PEP}$ in the presence of UDP-GlcNAc (*71*), and it hydrolyzes PEP in the absence of UDP-GlcNAc, albeit slowly. Thus, it is plausible that MurA-catalyzed arsenoenolpyruvate breakdown accounted for the lack of ^{18}O incorporation.

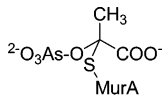

1

Thus, the mechanism of arsenate-promoted EP-UDP-GlcNAc hydrolysis was ambiguous. The ^2H and ^3H results demonstrated that MurA protonates and deprotonates C3′ in the arsenate-promoted reaction. The ^{18}O results were consistent with arsenate being a bystander in the reaction, i.e., direct water attack on EP-OR or its oxacarbenium ion, or with breakdown of the arsenoenolpyruvate product through C−O bond cleavage in an enzyme-catalyzed step. We note that the relative k_{cat}/K_M values for arsenate, vanadate, and fluorophosphate (Table 1) were similar with AroA and MurA, implying similar reaction pathways for both enzymes. Nonetheless, these data do not allow an unambiguous assignment of mechanism for the MurA reaction.

DISCUSSION

AroA- and MurA-catalyzed EP-OR hydrolysis is slow in the absence of phosphate, with k_{cat} values of $(4.7 \pm 0.5) \times 10^{-4}$ and $(4.2 \pm 0.4) \times 10^{-4}$ s^{-1}, respectively, compared with a literature value of 4.7×10^{-4} s^{-1} for AroA (*15*). The $\sim 10^5$-fold increase in rates upon phosphate binding does not arise from the inherent reactivity of phosphate with the enolpyruvyl group but rather from the enzymes using binding energy to promote reactivity. Phosphate is a modest nucleophile, weaker than or similar to acetate (*72*−*74*). Arsenate and vanadate are 6- and 900-fold more nucleophilic, respectively, than phosphate in the dianion form (*75*) but had 100- and 200-fold lower k_{cat}/K_M values, respectively, in AroA reactions. Thus, nucleophilicity was not the determining factor for reactivity with AroA and MurA. Phosphate desolvation upon binding in the active site would be expected to increase its nucleophilicity, though it is not clear how much, given its highly polar binding sites (*75*, *76*). Desolvation may drive conformational change and thus the observed fluorescence decrease associated with phosphate binding.

There is no good evidence for or against nucleophile activation, but there is good evidence for enolpyruvyl activation. In the forward reaction, AroA catalyzed solvent ^2H exchange at C3′ of PEP in the presence of 4,5-dideoxy-S3P, an S3P analogue lacking the nucleophilic hydroxyl (*12*). Presumably, ^2H exchange must occur through an oxacarbenium ion. In the reverse reaction, AroA forms EPSP ketal in the enzyme active site, evidence that it activates the enolpyruvyl group, forming an oxacarbenium ion, or a highly oxacarbenium ion-like transition state for hydroxyl addition (*77*).[2] Solvent ^2H exchange into EP-OR observed in this study is consistent with reversible oxacarbenium ion formation, but it is also consistent with reversible THI (or THI analogue) formation. The fact that there was little difference between K_{d,HPO_4} in the absence of EP-OR and K_{M,HPO_4} in the presence of EP-OR (*19*) implies that the enzymes are able to convert all of the phosphate binding energy into TS stabilization in the reverse reaction. Similarly, there was little difference in K_{d,HPO_4} in the presence and absence of EP-OR with $AroA_{H6}$_Asp313Ala.

Phosphate Analogues: Binding and EP-OR Activation. The same three phosphate analogues promoted EP-OR breakdown with both AroA and MurA, with similar relative specificity constants, i.e., $(k_{cat}/K_M)_{HPO_4}/(k_{cat}/K_M)_{analogue}$, of approximately 100 for arsenate, 200 for vanadate, and 5000 for fluorophosphate (Table 1). This similarity implies similar interactions of the phosphate analogues with both enzymes and similar catalytic mechanisms.

Comparison of the physicochemical properties of each analogue with their ability to bind and/or promote EP-OR

[2] M. E. Clark and P. J. Berti, unpublished data.

breakdown shed light on the factors that are important for catalysis. None of the nontetrahedral phosphate analogues (AlF_4^-,[3] HCO_3^-, or NO_3^-) interacted detectably with either enzyme, while all tetrahedral analogues bound to AroA, except for sulfate (see below). Thus, tetrahedral geometry was important but not sufficient for binding. Size was not an important factor for binding of the analogue alone, though binding of the largest two analogues, monomethyl phosphate and thiophosphate, was competitive with EPSP.

The overall charge in each phosphate analogue did not correlate with binding or reactivity. At the reaction pH, 7.5, the dianion form is dominant in phosphate and two reactive phosphate analogues, arsenate and fluorophosphate, and several nonreactive ones. The monoanion form was dominant in one reactive analogue, vanadate, and one unreactive analogue, methylphosphonic acid. Thus, there was no apparent correlation between either binding or reactivity and the overall charge on the phosphate analogues. Similarly, there was no apparent correlation with the charges on individual deprotonated oxygen atoms, calculated at the DFT level, which varied across a small range, from -0.9 to -1.3 (data not shown).

Sulfate was the only tetrahedral phosphate analogue that did not bind to $AroA_{H6}$. That this discrimination should occur is not surprising; sulfate is the only analogue that was tested that occurs in significant physiological concentrations, with intracellular concentrations in bacteria of $\sim$100 μM (*78*). The discrimination mechanism is not obvious given its similarity to phosphate in tetrahedral geometry, size, and overall charge. The major difference between HPO_4^{2-} and SO_4^{2-} is the lack of proton on sulfate at physiological pH. The lack of a proton on SO_4^{2-} has been proposed as the main way that some proteins distinguish between sulfate and phosphate (*79*). The hard or soft character of phosphate versus sulfate has also been proposed as a mechanism of distinguishing between them. With AroA, neither factor is likely to be definitive; tungstate bound to AroA despite having no proton at physiological pH, and arsenate was reactive despite being even softer than sulfate. Rather, a combination of factors appears to combine to discriminate against sulfate.

K_{d,WO_4} with AroA was similar to that with the active phosphate analogues, but tungstate did not promote EP-OR breakdown and did not cause solvent ^2H exchange in ^2H_2O (Table 1). This demonstrated that binding and catalysis were independent events. The lack of reactivity was likely due to a combination of the lack of a proton at physiological pH (see below) and the large size, as reflected in the W$-$O bond lengths of 1.77 Å, 0.27 Å longer than the P$-$O bonds in phosphate. Although there is no evidence that tungstate binding was competitive with EPSP, a small displacement of the enolpyruvyl group within the active site would be enough to prevent catalysis.

What factors were important in the three phosphate analogues that promoted EP-OR breakdown? Of the phosphate analogues that were not so large that they displaced EPSP ($MeOPO_3^{2-}$ and $HSPO_3^{2-}$) or possessed a hydrophobic group that caused extremely weak binding ($MePO_3^{2-}$), one factor that distinguished reactive (e.g., $HAsO_4^{2-}$ and $H_2VO_4^{2-}$) from nonreactive (e.g., SO_4^{2-} and WO_4^{2-}) phosphate analogues was the presence of at least one proton. If we assume that a proton is required for reactivity, then the [dianion]/[monoanion] ratio for SO_4^{2-}, 3×10^5, would ensure that it is unreactive. The ratio with FPO_3^{2-}, 500, would ensure its reactivity was low, despite otherwise very similar sizes, shapes, and charge distributions for it and phosphate. With WO_4^{2-}, presumably the combination of larger size and unfavorable [dianion]/[monoanion] ratio, 600, made it unreactive. The role of a proton in the mechanism is not clear. Presumably, general acid catalysis is required for elimination of R-OH from the THI; however, the proposed catalytic residue, Lys22 (*39*, *44*), would not necessarily require a proton from the phosphate analogue. Even given its unusually low pK_a, 7.6 (*80*), a significant fraction of Lys22 Nϵ would already be protonated in the free enzyme. In one proposed mechanism, phosphate deprotonates C3′ of the THI in the elimination step of the forward reaction (*38*). In the reverse reaction, phosphate would have to supply a proton to C3′. The requirement for a proton in phosphate analogues is consistent with this mechanism, though we have previously proposed that AroA_Glu341 deprotonates C3′, not phosphate (*44*). In AroA crystal structures (*11*, *39*), there are no side chains apparent that could directly accept a hydrogen bond from phosphate; however, a crystallographically conserved water would allow a bridged hydrogen bond to AroA_Asp49. Asp49 has been shown to be important for catalysis and is completely conserved in AroA and MurA sequences (*44*).

Mechanism of Arsenate-Promoted EP-OR Breakdown. The ^{18}O, ^3H, and ^2H labeling experiments demonstrated that the arsenate-promoted AroA reaction proceeded through an arseno-THI intermediate analogous to the normal catalytic intermediate. The ^3H and ^2H results demonstrated that AroA is able to protonate and deprotonate the methylene carbon, C3′. Incorporation of ^{18}O into arsenate demonstrated that it was involved in the chemical steps of the reaction, and not merely a bystander. This implies at least arseno-THI intermediate formation, but more likely aresenoenolpyruvate formation, because arseno-THI formation would not itself lead to breakdown of EP-OR to pyruvate and R-OH. For the MurA reaction, there was good evidence for activation of the methylene carbon, but the $H_2{}^{18}O$ experiments did not support direct participation of arsenate, though it cannot be ruled out.

Conformational Changes upon Ligand Binding. In addition to $K_{d,L}$, fluorescence titrations provided information about conformational changes. The crystal structures of both MurA and AroA demonstrate conformational changes upon binding substrates, intermediates, products, and some inhibitors (*30*, *81*). With AroA, the conformational change is a rigid-body rotation of the N- and C-terminal domains relative to each other, with little change in the structure of either domain. Ligand binding causes the two domains to move closer together (*11*), and this movement has been associated with the Trp fluorescence change.

In this study, phosphate and several analogues caused the fluorescence changes in tryptophan associated with conformational change. Fluorescence titrations with $AroA_{H6}$_D313A demonstrated that EPSP bound with a similar affinity to $AroA_{H6}$. This was somewhat surprising, as crystal structures indicated a potential 2.6$-$3.0 Å hydrogen bond between D313 and O4′H of S3P (*11*, *82*), fluoro-THI (*83*), and phosphonate analogues of the THI (*84*) which would be expected to promote S3P and EPSP binding. In the

[3] AlF_4^- solutions are actually a mixture of AlF_4^-, AlF_3, and $AlF_x(OH)_y$. The lack of an effect on the enzymes implies that none interacted appreciably with the enzymes.

AroA_D313A·THI structure, the position of the A313 backbone was unchanged, as was O4′H, indicating that the same hydrogen bond would be possible in the AroA·THI complex. The lack of an effect on $K_{d,EPSP}$ is consistent, however, with the observation that the D313A mutation has little effect on $K_{M,S3P}$ or $K_{M,PEP}$, even though it decreases k_{cat} dramatically.[4] Titration of the $AroA_{H6}$_D313A·EPSP complex with phosphate resulted in a further decrease in fluorescence. This provides evidence that AroA undergoes an additional conformational change upon phosphate binding, consistent with the idea that phosphate induces a change in the AroA·EPSP complex to activate the enolpyruvyl group. Titration of the $AroA_{H6}$_D131A·EPSP complex with arsenate also caused a fluorescence change (Figure 1b).

Oxacarbenium Ions. Enzymatic protonation of the EP-OR group would yield an oxacarbenium ion, the same intermediate that formed during acid-catalyzed EPSP hydrolysis, where C3′ protonation is rate-limiting (*85*). Protonation of carbon bases is difficult both thermodynamically and kinetically, with a large intrinsic barrier to proton transfer (*85*, *86*). Assuming that the pK_a of C3′ is less than −4, protonation at physiological pH would be disfavored by >15 kcal/mol. Nonetheless, AroA and MurA accomplish this protonation smoothly, as well as protonating C3′ of PEP in the forward reaction. Solvent ^2H exchange observed in this study in both the AroA and MurA reactions is further evidence for enolpyruvyl group activation. However, this impressive catalytic power is not expressed as soon as EP-OR enters the active site; it is increased ∼10^5-fold upon phosphate binding.

Implications for Inhibitor Design. MurA and AroA are potential antibiotic targets. The effectiveness of the existing inhibitors, fosfomycin, an antibiotic, and glyphosate, a herbicide, is limited by the fact that their anionic phosphonate groups prevent spontaneous transport across bacterial cell membranes. Fosfomycin is actively imported by sugar phosphate transporters in susceptible bacteria (*9*, *87*). Bacteria that do not misrecognize fosfomycin as a phosphorylated sugar are fosfomycin-resistant. Glyphosate is not an antibiotic, although it inhibits many bacterial AroAs, presumably because it is unable to cross the cell membranes. By understanding enzyme−phosphate interactions in detail, we may be able to design phosphonate-free inhibitors which take advantage of the naturally high intracellular phosphate concentrations in *E. coli*, 20 mM (*88*), to achieve tight binding. The fact that phosphate (and some analogues) causes the enzymes to activate the enolpyruvyl group by stabilizing an inherently unstable oxacarbenium ion implies that binding of good oxacarbenium mimics will be greatly enhanced by simultaneous binding of endogenous phosphate, without the requirement of transporting an anionic functional group across the cell membrane as part of the inhibitor.

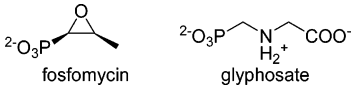

CONCLUSIONS

Eleven different phosphate analogues were used to study the reverse reactions of AroA and MurA with EP-OR. Many bound with the enzymes, but only arsenate, vanadate, and fluorophosphate were able to promote EP-OR breakdown, with arsenate being the most effective. Examination of the arsenate-promoted AroA reaction indicated that it proceeds through the normal reaction pathway, forming an arsenotetrahedral intermediate. The isotope labeling experiments gave ambiguous results with the arsenate-promoted MurA reaction. Fluorescence titrations of EPSP and phosphate binding to a mutant AroA, Asp313Ala, demonstrated a conformational change upon EPSP binding, followed by a further change upon phosphate binding.

[4] P. Chindemi and P. J. Berti, unpublished results.

ACKNOWLEDGMENT

We thank Dr. Paul Loncke for help with computations and Paul Chindemi for determining K_{M,H_2VO_4}.

REFERENCES

1. Anderson, K. S., and Johnson, K. A. (1990) Kinetic and structural analysis of enzyme intermediates: Lessons from EPSP synthase, *Chem. Rev. 90*, 1131−1149.
2. Anderson, K. S., Sammons, R. D., Leo, G. C., Sikorski, J. A., Benesi, A. J., and Johnson, K. A. (1990) Observation by ^{13}C NMR of the EPSP synthase tetrahedral intermediate bound to the enzyme active site, *Biochemistry 29*, 1460−1465.
3. Gunetileke, K. G., and Anwar, R. A. (1968) Biosynthesis of uridine diphospho-*N*-acetylmuramic acid. II. Purification and properties of pyruvate-uridine diphospho-*N*-acetylglucosamine transferase and characterization of uridine diphospho-*N*-acetylenopyruvylglucosamine, *J. Biol. Chem. 243*, 5770−5778.
4. Walsh, C. T., Benson, T. E., Kim, D. H., and Lees, W. J. (1996) The versatility of phosphoenolpyruvate and its vinyl ether products in biosynthesis, *Chem. Biol. 3*, 83−91.
5. Schmid, J., and Amrhein, N. (1999) in *Plant Amino Acids: Biochemistry and Biotechnology* (Singh, B., Ed.) pp 147−169, Marcel Dekker, New York.
6. Sikorski, J. A., and Gruys, K. J. (1997) Understanding glyphosate's molecular mode of action with EPSP synthase: Evidence for an allosteric inhibitor model, *Acc. Chem. Res. 30*, 2−8.
7. Bugg, T. D., and Walsh, C. T. (1992) Intracellular steps of bacterial cell wall peptidoglycan biosynthesis: Enzymology, antibiotics, and antibiotic resistance, *Nat. Prod. Rep. 9*, 199−215.
8. Alibhai, M. F., and Stallings, W. C. (2001) Closing down on glyphosate inhibition with a new structure for drug discovery, *Proc. Natl. Acad. Sci. U.S.A. 98*, 2944−2946.
9. Kahan, F. M., Kahan, J. S., Cassidy, P. J., and Kropp, H. (1974) Mechanism of action of fosfomycin (phosphonomycin), *Ann. N.Y. Acad. Sci. 235*, 364−386.
10. Schonbrunn, E., Sack, S., Eschenburg, S., Perrakis, A., Krekel, F., Amrhein, N., and Mandelkow, E. (1996) Crystal structure of UDP-*N*-acetylglucosamine *enol*pyruvyltransferase, the target of the antibiotic fosfomycin, *Structure 4*, 1065−1075.
11. Schonbrunn, E., Eschenburg, S., Shuttleworth, W. E., Schloss, J. V., Amrhein, N., Evans, J. N. S., and Kabsch, W. (2001) Interaction of the herbicide glyphosate with its target enzyme 5-enolpyruvylshikimate 3-phosphate synthase in atomic detail, *Proc. Natl. Acad. Sci. U.S.A. 98*, 1376−1380.
12. Anton, D. L., Hedstrom, L., Fish, S., and Abeles, R. H. (1983) Mechanism of enolpyruvylshikimate-3-phosphate synthase exchange of phosphoenolpyruvate with solvent protons, *Biochemistry 22*, 5903−5908.
13. Anderson, K. S., Sikorski, J. A., Benesi, A. J., and Johnson, K. A. (1988) Isolation and structural elucidation of the tetrahedral intermediate in the EPSP synthase enzymic pathway, *J. Am. Chem. Soc. 110*, 6577−6579.
14. Anderson, K. S., Sikorski, J. A., and Johnson, K. A. (1988) Evaluation of 5-enolpyruvoylshikimate-3-phosphate synthase substrate and inhibitor binding by stopped-flow and equilibrium fluorescence measurements, *Biochemistry 27*, 1604−1610.
15. Anderson, K. S., Sikorski, J. A., and Johnson, K. A. (1988) A tetrahedral intermediate in the EPSP synthase reaction observed by rapid quench kinetics, *Biochemistry 27*, 7395−7406.
16. Anderson, K. S., and Johnson, K. A. (1990) "Kinetic competence" of the 5-enolpyruvoylshikimate-3-phosphate synthase tetrahedral intermediate, *J. Biol. Chem. 265*, 5567−5572.

17. Stallings, W. C., Abdel-Meguid, S. S., Lim, L. W., Shieh, H.-S., Dayringer, H. E., Leimgruber, N. K., Stegeman, R. A., Anderson, K. S., Sikorski, J. A., Padgette, S. R., and Kishore, G. H. (1991) Structure and topological symmetry of the glyphosate target 5-enol-pyruvylshikimate-3-phosphate synthase: A distinctive protein fold, *Proc. Natl. Acad. Sci. U.S.A. 88*, 5046−5050.
18. Marquardt, J. L., Brown, E. D., Walsh, C. T., and Anderson, K. S. (1993) Isolation and structural elucidation of a tetrahedral intermediate in the UDP-*N*-acetylglucoamine enolpyruvyl transferase enzymatic pathway, *J. Am. Chem. Soc. 115*, 10398−10399.
19. Gruys, K. J., Marzabadi, M. R., Pansegrau, P. D., and Sikorski, J. A. (1993) Steady-state kinetic evaluation of the reverse reaction for *Escherichia coli* 5-*enol*pyruvoylshikimate-3-phosphate synthase, *Arch. Biochem. Biophys. 304*, 345−351.
20. Marquardt, J. L., Brown, E. D., Lane, W. S., Haley, T. M., Ichikawa, Y., Wong, C. H., and Walsh, C. T. (1994) Kinetics, stoichiometry, and identification of the reactive thiolate in the inactivation of UDP-GlcNAc *enol*pyruvoyl transferase by the antibiotic fosfomycin, *Biochemistry 33*, 10646−10651.
21. Brown, E. D., Marquardt, J. L., Lee, J. P., Walsh, C. T., and Anderson, K. S. (1994) Detection and characterization of a phospholactoyl-enzyme adduct in the reaction catalyzed by UDP-*N*-acetylglucosamine enolpyruvoyl transferase, MurZ, *Biochemistry 33*, 10638−10645.
22. Kim, D. H., Lees, W. J., and Walsh, C. T. (1994) Formation of two enzyme-bound reaction intermediate analogs during inactivation of UDP-GlcNAc enolpyruvyl transferase by (*E*)- or (*Z*)-3-fluorophosphoenolpyruvate, *J. Am. Chem. Soc. 116*, 6478−6479.
23. Kim, D. H., Lees, W. J., and Walsh, C. T. (1995) Stereochemical analysis of the tetrahedral adduct formed at the active site of UDP-GlcNAc enolpyruvyl transferase from the pseudosubstrates, (*E*)- and (*Z*)-3-fluorophosphoenolpyruvate, in D_2O, *J. Am. Chem. Soc. 117*, 6380−6381.
24. Kim, D. H., Lees, W. J., Haley, T. M., and Walsh, C. T. (1995) Kinetic characterization of the inactivation of UDP-GlcNAc enolpyruvyl transferase by (*Z*)-3-fluorophosphoenolpyruvate: Evidence for two oxocarbenium ion intermediates in enolpyruvyl transfer catalysis, *J. Am. Chem. Soc. 117*, 1494−1502.
25. Lees, W. J., and Walsh, C. T. (1995) Analysis of the enol ether transfer catalyzed by UDP-GlcNAc *enol*pyruvyl transferase using (*E*)- and (*Z*)-isomers of phospho*enol*butyrate: Stereochemical, partitioning, and isotope effect studies, *J. Am. Chem. Soc. 117*, 7329−7337.
26. Sammons, R. D., Gruys, K. J., Anderson, K. S., Johnson, K. A., and Sikorski, J. A. (1995) Reevaluating glyphosate as a transition-state inhibitor of EPSP synthase: Identification of an EPSP synthase·EPSP·glyphosate ternary complex, *Biochemistry 34*, 6433−6440.
27. Kim, D. H., Tucker-Kellogg, G. W., Lees, W. J., and Walsh, C. T. (1996) Analysis of fluoromethyl group chirality establishes a common stereochemical course for the enolpyruvyl transfers catalyzed by EPSP synthase and UDP-GlcNAc enolpyruvyl transferase, *Biochemistry 35*, 5435−5440.
28. Kim, D. H., Lees, W. J., Kempsell, K. E., Lane, W. S., Duncan, K., and Walsh, C. T. (1996) Characterization of a Cys115 to Asp substitution in the *Escherichia coli* cell wall biosynthetic enzyme UDP-GlcNAc *enol*pyruvyl transferase (MurA) that confers resistance to inactivation by the antibiotic fosfomycin, *Biochemistry 35*, 4923−4928.
29. Paiva, A. A., Tilton, R. F., Crooks, G. P., Huang, L. Q., and Anderson, K. S. (1997) Detection and identification of transient enzyme intermediates using rapid mixing, pulsed-flow electrospray mass spectrometry, *Biochemistry 36*, 15472−15476.
30. Schonbrunn, E., Svergun, D. I., Amrhein, N., and Koch, M. H. (1998) Studies on the conformational changes in the bacterial cell wall biosynthetic enzyme UDP-*N*-acetylglucosamine *enol*pyruvyltransferase (MurA), *Eur. J. Biochem. 253*, 406−412.
31. Skarzynski, T., Kim, D. H., Lees, W. J., Walsh, C. T., and Duncan, K. (1998) Stereochemical course of enzymatic enolpyruvyl transfer and catalytic conformation of the active site revealed by the crystal structure of the fluorinated analogue of the reaction tetrahedral intermediate bound to the active site of the C115A mutant of MurA, *Biochemistry 37*, 2572−2577.
32. Lewis, J., Johnson, K. A., and Anderson, K. S. (1999) The catalytic mechanism of EPSP synthase revisited, *Biochemistry 38*, 7372−7379.
33. Shuttleworth, W. A., Pohl, M. E., Helms, G. L., Jakeman, G. L., and Evans, J. N. S. (1999) Site-directed mutagenesis of putative active site residues of 5-enolpyruvylshikimate-3-phosphate synthase, *Biochemistry 38*, 296−302.
34. Schonbrunn, E., Eschenburg, S., Krekel, F., Luger, K., and Amrhein, N. (2000) Role of the loop containing residue 115 in the induced-fit mechanism of the bacterial cell wall biosynthetic enzyme MurA, *Biochemistry 39*, 2164−2173.
35. Krekel, F., Samland, A. K., Macheroux, P., Amrhein, N., and Evans, J. N. (2000) Determination of the pK_a value of C115 in MurA (UDP-*N*-acetylglucosamine enolpyruvyltransferase) from *Enterobacter cloacae*, *Biochemistry 39*, 12671−12677.
36. Eschenburg, S., and Schonbrunn, E. (2000) Comparative X-ray analysis of the un-liganded fosfomycin-target MurA, *Proteins 40*, 290−298.
37. Stauffer, M. E., Young, J. K., and Evans, J. N. (2001) Shikimate-3-phosphate binds to the isolated N-terminal domain of 5-enolpyruvylshikimate-3-phosphate synthase, *Biochemistry 40*, 3951−3957.
38. An, M., Maitra, U., Neidlein, U., and Bartlett, P. A. (2003) 5-Enolpyruvylshikimate 3-phosphate synthase: Chemical synthesis of the tetrahedral intermediate and assignment of the stereochemical course of the enzymatic reaction, *J. Am. Chem. Soc. 125*, 12759−12767.
39. Eschenburg, S., Kabsch, W., Healy, M. L., and Schonbrunn, E. (2003) A new view of the mechanisms of UDP-*N*-acetylglucosamine *enol*pyruvyl transferase (MurA) and 5-*enol*pyruvylshikimate-3-phosphate synthase (AroA) derived from X-ray structures of their tetrahedral reaction intermediate states, *J. Biol. Chem. 278*, 49215−49222.
40. Priestman, M. A., Funke, T., Singh, I. M., Crupper, S. S., and Schonbrunn, E. (2005) 5-Enolpyruvylshikimate-3-phosphate synthase from *Staphylococcus aureus* is insensitive to glyphosate, *FEBS Lett. 579*, 728−732.
41. Eschenburg, S., Priestman, M., and Schonbrunn, E. (2005) Evidence that the fosfomycin target Cys115 in UDP-*N*-acetylglucosamine enolpyruvyl transferase (MurA) is essential for product release, *J. Biol. Chem. 280*, 3757−3763.
42. Eschenburg, S., Priestman, M. A., Abdul-Latif, F. A., Delachaume, C., Fassy, F., and Schonbrunn, E. (2005) A novel inhibitor that suspends the induced fit mechanism of UDP-*N*-acetylglucosamine enolpyruvyl transferase (MurA), *J. Biol. Chem. 280*, 14070−14075.
43. Mizyed, S., Oddone, A., Byczynski, B., Hughes, D. W., and Berti, P. J. (2005) UDP-*N*-acetylmuramic acid (UDP-MurNAc) is a potent inhibitor of MurA (*enol*pyruvyl-UDP-GlcNAc synthase), *Biochemistry 44*, 4011−4017.
44. Mizyed, S., Wright, J. E. I., Byczynski, B., and Berti, P. J. (2003) Identification of the catalytic residues of AroA (*enol*pyruvylshikimate 3-phosphate synthase) using partitioning analysis, *Biochemistry 42*, 6986−6995.
45. Byczynski, B., Mizyed, S., and Berti, P. J. (2003) Nonenzymatic breakdown of the tetrahedral (α-carboxyketal phosphate) intermediates of MurA and AroA, two carboxyvinyl transferases. Protonation of different functional groups controls the rate and fate of breakdown, *J. Am. Chem. Soc. 125*, 12541−12550.
46. Gruys, K. J., Walker, M. C., and Sikorski, J. A. (1992) Substrate synergism and the steady-state kinetic reaction mechanism for EPSP synthase from *Escherichia coli*, *Biochemistry 31*, 5534−5544.
47. Gordon, J. A. (1991) Use of vanadate as protein-phosphotyrosine phosphatase inhibitor, *Methods Enzymol. 201*, 477−482.
48. Fauman, E. B., Yuvaniyama, C., Schubert, H. L., Stuckey, J. A., and Saper, M. A. (1996) The X-ray crystal structures of *Yersinia* tyrosine phosphatase with bound tungstate and nitrate. Mechanistic implications, *J. Biol. Chem. 271*, 18780−18788.
49. Stuckey, J. A., Schubert, H. L., Fauman, E. B., Zhang, Z. Y., Dixon, J. E., and Saper, M. A. (1994) Crystal structure of *Yersinia* protein tyrosine phosphatase at 2.5 Å and the complex with tungstate, *Nature 370*, 571−575.
50. Voegtli, W. C., White, D. J., Reiter, N. J., Rusnak, F., and Rosenzweig, A. C. (2000) Structure of the bacteriophage lambda Ser/Thr protein phosphatase with sulfate ion bound in two coordination modes, *Biochemistry 39*, 15365−15374.
51. Rose, Z. B., and Liebowitz, J. (1970) 2,3-Diphosphoglycerate phosphatase from human erythrocytes. General properties and activation by anions, *J. Biol. Chem. 245*, 3232−3241.
52. Egloff, M. P., Cohen, P. T., Reinemer, P., and Barford, D. (1995) Crystal structure of the catalytic subunit of human protein phosphatase 1 and its complex with tungstate, *J. Mol. Biol. 254*, 942−959.

53. Coleman, D. E., Berghuis, A. M., Lee, E., Linder, M. E., Gilman, A. G., and Sprang, S. R. (1994) Structures of active conformations of $G_{i\alpha1}$ and the mechanism of GTP hydrolysis, *Science 265*, 1405−1412.
54. Phillips, D. R., and Fife, T. H. (1969) Steric effects in the glyceraldehyde 3-phosphate dehydrogenase catalyzed hydrolysis of acyl phosphates. An example of substrate-induced cooperativity, *Biochemistry 8*, 3114−3119.
55. Long, J. W., and Ray, W. J., Jr. (1973) Kinetics and thermodynamics of the formation of glucose arsenate. Reaction of glucose arsenate with phosphoglucomutase, *Biochemistry 12*, 3932−3937.
56. Kline, P. C., and Schramm, V. L. (1993) Purine nucleoside phosphorylase. Catalytic mechanism and transition-state analysis of the arsenolysis reaction, *Biochemistry 32*, 13212−13219.
57. Mao, C., Cook, W. J., Zhou, M., Federov, A. A., Almo, S. C., and Ealick, S. E. (1998) Calf spleen purine nucleoside phosphorylase complexed with substrates and substrate analogues, *Biochemistry 37*, 7135−7146.
58. Nidetzky, B., and Eis, C. (2001) α-Retaining glucosyl transfer catalysed by trehalose phosphorylase from *Schizophyllum commune*: Mechanistic evidence obtained from steady-state kinetic studies with substrate analogues and inhibitors, *Biochem. J. 360*, 727−736.
59. Eis, C., and Nidetzky, B. (2002) Substrate-binding recognition and specificity of trehalose phosphorylase from *Schizophyllum commune* examined in steady-state kinetic studies with deoxy and deoxyfluoro substrate analogues and inhibitors, *Biochem. J. 363*, 335−340.
60. Silverstein, R., Voet, J., Reed, D., and Abeles, R. H. (1967) Purification and mechanism of action of sucrose phosphorylase, *J. Biol. Chem. 242*, 1338−1346.
61. Schoevaart, R., van Rantwijk, F., and Sheldon, R. A. (2001) Facile enzymatic aldol reactions with dihydroxyacetone in the presence of arsenate, *J. Org. Chem. 66*, 4559−4562.
62. Byers, L. D., She, H. S., and Alayoff, A. (1979) Interaction of Phosphate Analogs with Glyceraldehyde-3-Phosphate Dehydrogenase, *Biochemistry 18*, 2471−2480.
63. Duggleby, R. G. (1983) Determination of the kinetic properties of enzymes catalysing coupled reaction sequences, *Biochim. Biophys. Acta 744*, 249−259.
64. Kumler, W. D., and Eiler, J. J. (1943) The acid strength of mono and diesters of phosphoric acid. The *n*-alkyl esters from Me to Bu, the esters of biological importance and the natural guanidinephosphoric acids, *J. Am. Chem. Soc. 65*, 2355−2361.
65. Bailey, N., Carrington, A., Lott, K. A. K., and Symons, M. C. R. (1960) Structure and reactivity of the oxyanions of transition metals. VIII. Acidities and spectra of protonated oxyanions, *J. Chem. Soc., Abstr.*, 290−297.
66. Bjerrum, J., Schwarzenbach, G., Sillen, L. G., Berecki-Biedermann, C., Maltesen, L., Rasmussen, S. E., and Rossotti, F. J. C. (1958) *Stability constants of metal-ion complexes, with solubility products of inorganic substances. II. Inorganic ligands with solubility products of inorganic substances*, Vol. 7, Chemical Society, London.
67. Crofts, P. C., and Kosolapoff, G. M. (1953) Preparation and determination of apparent dissociation constants of some alkylphosphonic and dialkylphosphinic acids, *J. Am. Chem. Soc. 75*, 3379−3383.
68. Lagunas, R., and Solis, A. (1968) Arsenate induced activity of certain enzymes on their dephosphorylated subtrates, *FEBS Lett. 1*, 32−34.
69. Grimshaw, C. E., Sogo, S. G., and Knowles, J. R. (1982) The fate of the hydrogens of phosphoenolpyruvate in the reaction catalyzed by 5-enolpyruvylshikimate-3-phosphate synthase. Isotope effects and isotope exchange, *J. Biol. Chem. 257*, 596−598.
70. Bondinell, W. E., Vnek, J., Knowles, P. F., Sprecher, M., and Sprinson, D. B. (1971) On the mechanism of 5-enolpyruvylshikimate 3-phosphate synthetase, *J. Biol. Chem. 246*, 6191−6196.
71. Marquardt, J. L. (1993) Ph.D. Thesis, pp 187, Harvard University, Cambridge, MA.
72. Herschlag, D., and Jencks, W. P. (1989) Phosphoryl Transfer to Anionic Oxygen Nucleophiles: Nature of the Transition-State and Electrostatic Repulsion, *J. Am. Chem. Soc. 111*, 7587−7596.
73. Kovach, I. M., Bennet, A. J., Bibbs, J. A., and Zhao, Q. J. (1993) Nucleophilic and Protolytic Catalysis of Phosphonate Hydrolysis: Isotope Effects and Activation Parameters, *J. Am. Chem. Soc. 115*, 5138−5144.
74. El Seoud, O. A., Ruasse, M.-F., and Rodrigues, W. A. (2002) Kinetics and mechanism of phosphate-catalyzed hydrolysis of benzoate esters: Comparison with nucleophilic catalysis by imidazole and *o*-iodosobenzoate, *J. Chem. Soc., Perkin Trans. 2*, 1053−1058.
75. Rucker, V. C., and Byers, L. D. (2000) An assessment of desolvation on rates of acetyl transfer: Insights into enzyme catalysis, *J. Am. Chem. Soc. 122*, 8365−8369.
76. Jencks, W. P. (1975) Binding energy, specificity, and enzymic catalysis: The Circe effect, *Adv. Enzymol. Relat. Areas Mol. Biol. 43*, 219−410.
77. Leo, G. C., Sikorski, J. A., and Sammons, R. D. (1990) Novel product from EPSP synthase at equilibrium, *J. Am. Chem. Soc. 112*, 1653−1654.
78. Dreyfuss, J. (1964) Characterization of a sulfate- and thiosulfate-transporting system in *Salmonella typhimurium*, *J. Biol. Chem. 239*, 2292−2297.
79. O'Brien, P. J., and Herschlag, D. (2002) Alkaline phosphatase revisited: Hydrolysis of alkyl phosphates, *Biochemistry 41*, 3207−3225.
80. Huynh, Q. K., Kishore, G. M., and Bild, G. S. (1988) 5-Enolpyruvyl shikimate 3-phosphate synthase from *Escherichia coli*. Identification of Lys-22 as a potential active site residue, *J. Biol. Chem. 263*, 735−739.
81. Krekel, F., Oecking, C., Amrhein, N., and Macheroux, P. (1999) Substrate and inhibitor-induced conformational changes in the structurally related enzymes UDP-*N*-acetylglucosamine enolpyruvyl transferase (MurA) and 5-enolpyruvylshikimate 3-phosphate synthase (EPSPS), *Biochemistry 38*, 8864−8878.
82. Eschenburg, S., Healy, M. L., Priestman, M. A., Lushington, G. H., and Schonbrunn, E. (2002) How the mutation glycine96 to alanine confers glyphosate insensitivity to 5-enolpyruvyl shikimate-3-phosphate synthase from *Escherichia coli*, *Planta 216*, 129−135.
83. Park, H., Hilsenbeck, J. L., Kim, H. J., Shuttleworth, W. A., Park, Y. H., Evans, J. N., and Kang, C. (2004) Structural studies of *Streptococcus pneumoniae* EPSP synthase in unliganded state, tetrahedral intermediate-bound state and S3P-GLP-bound state, *Mol. Microbiol. 51*, 963−971.
84. Priestman, M. A., Healy, M. L., Becker, A., Alberg, D. G., Bartlett, P. A., Lushington, G. H., and Schonbrunn, E. (2005) Interaction of phosphonate analogues of the tetrahedral reaction intermediate with 5-enolpyruvylshikimate-3-phosphate synthase in atomic detail, *Biochemistry 44*, 3241−3248.
85. Kresge, A. J., Leibovitch, M., and Sikorski, J. A. (1992) Acid-catalyzed hydrolysis of 5-enolpyruvylshikimate 3-phosphate (EPSP) and some simple models of its vinyl ether functional group, *J. Am. Chem. Soc. 114*, 2618−2622.
86. Richard, J. P., Amyes, T. L., and Williams, K. B. (1998) Intrinsic barriers to the formation and reaction of carbocations, *Pure Appl. Chem. 70*, 2007−2014.
87. Nilsson, A. I., Berg, O. G., Aspevall, O., Kahlmeter, G., and Andersson, D. I. (2003) Biological costs and mechanisms of fosfomycin resistance in *Escherichia coli*, *Antimicrob. Agents Chemother. 47*, 2850−2858.
88. Roberts, R. B., Cowie, D. B., Abelson, P. H., Bolton, E. T., and Britten, R. J. (1963) *Studies of biosynthesis in Escherichia coli*, Publication 607, Carnegie Institution of Washington, Washington, DC.

BI0601914